Electrochemically Driven Ion Insertion Processes across Liquid|Liquid Boundaries: Neutral versus Ionic Redox Liquids

Uwe Schröder, Richard G. Compton, and Frank Marken*,†

Physical & Theoretical Chemistry Laboratory, Oxford University, South Parks Road, Oxford OX1 3QZ, U.K.

Steven D. Bull and Stephen G. Davies

Dyson Perrins Laboratory, Oxford University, South Parks Road, Oxford OX1 3QY, U.K.

Sandra Gilmour

Sharp Laboratories of Europe Ltd., Edmund Halley Road, Oxford Science Park, Oxford OX4 4GA, U.K.

Received: October 2, 2000; In Final Form: November 28, 2000

The oxidation and rereduction of the redox liquids *para*-*N*,*N*,*N*′,*N*′-tetrahexylphenylenediamine (THPD) and *para*-*N*,*N*,*N*′-trihexylphenylenediamine (TriHPD) associated with anion and proton insertion and expulsion are studied as a function of the proton concentration in aqueous $NaClO_4$ electrolyte. Voltammetric, in situ UV/vis-spectroelectrochemical, and quartz crystal microbalance techniques are employed. The biphasic acid−base equilibria of the redox liquids involving protonation and simultaneous anion transfer from the aqueous phase are shown to exhibit only small deviation from ideal behavior and well-defined biphasic dissociation constants, $pK_{A,biphasic}$ have been determined. However, the protonation of the bulk redox liquids is shown to be dominated by intermolecular rather than intramolecular factors. In particular, the ability of THPD to undergo bulk protonation by $HClO_4$ is higher ($pK_{A2,biphasic} = 5.1$) compared to that of TriHPD ($pK_{A2,biphasic} = 3.9$); this is *opposite* to the behavior predicted on the basis of the estimated values for the aqueous protonation equilibrium constants, $pK_{A2} = 7.5 \pm 0.5$ and $pK_{A2} = 8.8 \pm 0.5$ for THPD and TriHPD, respectively. Further, the electrochemically driven deprotonation occurs irrespective of protonation constants at essentially the same potential for both materials. The three-phase junction electrode|redox liquid|aqueous electrolyte for the initiation of the anion and proton insertion−electrochemical reactions is shown to be the key to processes observed for neutral redox liquids, whereas ionic redox liquids show reactivity independent of the three-phase junction due to sufficient ionic bulk conductivity.

Introduction

Electrochemically induced redox processes of liquid or solid compounds accompanied by the simultaneous transfer of ions from the adjacent electrolyte solution are of fundamental interest[1−4] and of importance for various potential applications, such as energy storage,[5] charge storage,[6] or ion sensing and detection.[7] Recent studies on neutral redox liquids have shown that, for example, the water insoluble N^1-[4-(dihexylamino)-phenyl]-N^1,*N*,$^4N^4$-trihexyl-1,4-phenylenediamine may serve as a system for sulfide detection.[8] The redox liquid *para*-*N*,*N*,*N*′,*N*′-tetrahexylphenylenediamine (THPD) has been studied extensively as a model system for electrochemically driven ion exchange[9] and was found to be a promising model system for the detection of some anionic species.[10] Further, the distinct electrochromism[9] and interesting photoelectrochemical behavior of THPD[11] have been reported.

In this study two redox liquids, *para*-*N*,*N*,*N*′,*N*′-tetrahexylphenylenediamine (THPD) and *para*-*N*,*N*,*N*′-trihexylphenylenediamine (TriHPD), are investigated with respect to their ability to undergo electrochemically driven anion and proton exchange with the surrounding aqueous solution phase. Experimentally, the work is based on deposition of the redox liquids in form of microdroplets or thin films onto basal plane pyrolytic graphite or gold electrodes followed by immersion into the aqueous electrolyte, equilibration, and redox cycling.

Both redox liquids, THPD and TriHPD, are easily protonated (eq 1) in the presence of an aqueous acid,[10] and the resulting ionic redox liquids exhibit electrochemical properties distinctly different from those of the neutral redox liquids. For THPD immersed in form of microdroplets in aqueous electrolyte, the first protonation (see eq 1) is followed by a second protonation at lower pH. Ionic conductivity in ionic redox liquids is shown

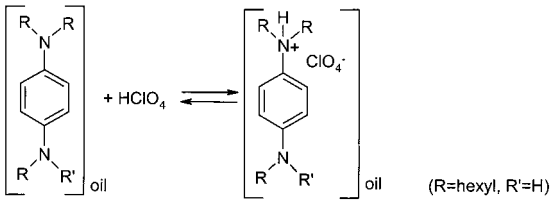

(1)

to change the electrochemical process from being governed by a triple interface reaction to following ion exchange via the entire liquid|liquid interface. This result is discussed in view of applications in energy storage and electrochromic systems.

* Corresponding author. Tel.: U.K. (0) 1509 22 2551. Fax: U.K. (0) 1509 22 3925. E-mail: F.Marken@lboro.ac.uk.

† Present address: Department of Chemistry, Loughborough University, Loughborough LE11 3TU, U.K.

10.1021/jp0035840 CCC: $20.00
Published on Web 01/25/2001

Experimental Section

Chemical Reagents. Aqueous electrolyte solutions have been prepared with $NaClO_4$ (Aldrich), NaOH (BDH), and perchloric acid (70%, Aldrich). Chemical reagents were of analytical or the purest commercially available grade. Deionized water was taken from an Elgastat filter system (Elga, Bucks, U.K.) and had a resistivity of not less than 18 MΩ cm. Nafion perfluorinated ion-exchange powder was used as a 5 wt % alcoholic solution as purchased from Aldrich.

para-N,N,N′,N′-Tetrahexylphenylene diamine (THPD) was prepared by following a literature procedure.[9] The formation of *para-N,N,N′*-trihexylphenylene diamine (TriHPD), which is a side product in the synthesis of *para-N,N,N′,N′*-tetrahexylphenylenediamine, has been reported recently.[9] This material was obtained in pure form after column chromatography with the following spectroscopic characteristics. ^{1}H NMR (200 MHz in $CDCl_3$, ppm): 0.90, brt m, 9H, CH_2CH_3; 1.30, brt, m, 18H, $NCH_2CH_2(CH_2)_3CH_3$, 1.54, brt, m, 4H, $N(CH_2CH_2(CH_2)_3CH_3)_2$; 1.93, brt, m, 2H, $NHCH_2CH_2(CH_2)_3CH_3$; 3.0−3.7, brt, m, 7H, NCH_2 and NH; 6.5−7.0, brt, m, 4H, Ar-*H*.

Instrumentation. Electrochemical experiments were conducted with a μ-Autolab system (Ecochemie, The Netherlands) in a conventional three-electrode cell. Special care was taken to avoid distortion of voltammetric signals due to the staircase mode. Only for potential steps smaller than 0.2 mV was reliable signal sampling observed. The electrodes used were a platinum gauze as the counter electrode and a saturated calomel electrode (Radiometer, Copenhagen) as the reference. This type of reference electrode is sensitive to high concentrations of ClO_4^-, but the resulting potential drift was minimized by short exposure times. The working electrode was a 4.9 mm diameter basal plane pyrolytic graphite disk mounted in a Teflon holder. Before and after electrochemical experiments the electrode surface was cleaned by rinsing with acetonitrile and occasionally renewed by polishing on a fine carborundum paper. The deposition of microdroplets of organic materials was achieved by solvent evaporation using a 0.5 mM solution of the organic precursors in acetonitrile. Unless otherwise stated experiments have been undertaken under an inert atmosphere of argon (BOC) and at a temperature of 20 ± 2 °C.

Spectroelectrochemical Measurements. A S2000/PC2000 miniature fiber optic spectrometer with a spectral resolution of 3 pixel/nm was utilized for the spectroelectrochemical measurements. An intense halogen lamp (FO 150, Chiu Technical Corp., NY) served as a light source. Poor wetting properties of THPD and TriHPD on electrode materials such as platinum, gold, and indium−tin oxide resulted in a less well-defined processes. Therefore and in order to use similar conditions for voltammetric and in situ spectroelectrochemical measurements, a planar pyrolytic carbon plate electrode (7 × 7 mm size) was employed for monitoring the changes of the reflectance and the optical absorption properties of the oil deposits. For the spectroelectrochemical measurement about 20 nmol of the redox liquid was transferred onto the electrode surface by solvent evaporation as described above. The electrode was then mounted in a glass cell containing reference and counter electrode. Light source, electrode, and light receiver (light guide cable) were arranged in a 45° angle toward the electrode surface ($_{45}R_{45}$), which allowed a maximum of light intensity to be received by the spectrometer. The voltammetric measurements (performed with the Autolab system described above) and the spectroscopic measurements were triggered simultaneously.

Electrochemical Quartz Crystal Microbalance (EQCM) Measurements. EQCM measurements[12] were performed using a μ-Autolab (Eco-Chemie, Utrecht, The Netherlands) combined with a Fluke PM6680B frequency counter (Fluke, The Netherlands) and a 10 MHz oscillator Model 230 with conventional AT-cut gold coated plano-convex quartz crystals (Technical Department, Institut Chemii Fizycznej Polskiej Akademii Nauk, Poland). EQCM measurements were undertaken to support interpretation of the nature of the ion insertion process. Results have been analyzed on the basis of the Sauerbrey equation.[13] However, data were interpreted with caution because changes of the viscosity of the redox liquid may contribute to the frequency change of the quartz crystal.[10]

Imprint Experiments. To visualize the spatial distribution of the reaction front within the oil deposit at the basal plane pyrolytic graphite electrode surface the following indirect method of creation of an imprint of the electrode surface after reaction was employed. In the first step a volume of approximately 0.5 μL of the pure redox liquid was transferred onto the surface of a planar pyrolytic carbon electrode (diameter 4.9 mm) in order to obtain a deposition of a continuous film of about 25 μm thickness instead of a microdroplet deposition. The electrode was then immersed into the electrolyte solution, and an appropriate oxidation potential was applied for the formation of the radical cations. The potential was held for 10−120 s in order to achieve a partial electrolysis of the layer. Next, the electrode was disconnected and the film was transferred onto the surface of a filter paper as an imprint. This transfer is necessary as the contrast between the graphite surface and the strongly light absorbing radical cations does not allow one to clearly distinguish between starting material and reaction product. Before the actual imprint is taken the unconverted top layers of the deposits were carefully removed. The electrode surface was pressed onto the filter paper (Whatman, type 1) after wetting the surface with little acetonitrile. A single lens reflex camera (Canon EOS, with a Kodak print film) was then utilized to take a picture of the imprint. For the presentation the picture was digitalized and transformed into a gray-scale image.

Values for the activity of ionic species in the aqueous electrolyte solutions were calculated from the concentration values (for up to 0.1 M solutions) using the extended Debye−Hückel law.

Results and Discussion

1. Electrochemically Driven Ion Insertion in Tetra- and Trihexylphenylenediamine Redox Liquids in the Absence of Acid. Provided a sufficiently fast mechanism for mass transport is operative, ion insertion and expulsion processes between two phases, e.g. an aqueous electrolyte and a neutral organic liquid, may be driven electrochemically at the triple interface.[14] It has been shown previously[15] that in the three-phase junction region electrode|redox liquid|aqueous electrolyte of this type of system the redox process can be initiated, and the subsequent need to maintain charge neutrality then drives the ion exchange between the two liquid phases.

Figure 1 shows cyclic voltammograms for the reversible ClO_4^- anion insertion and expulsion during oxidation and reduction of deposits of (A) 1.5 μg (3.5 nmol) of tetrahexylphenylenediamine (THPD) and (B) 1.5 μg (4 nmol) of trihexylphenylenediamine (TriHPD) in the presence of aqueous 1 M $NaClO_4$ (pH 7.5). The redox liquids have been deposited in form of microdroplets onto a basal plane pyrolytic graphite electrode prior to the electrochemical study (see Experimental Section) and are then immersed into the aqueous electrolyte. As shown previously[9] oxidation accompanied by anion uptake from the

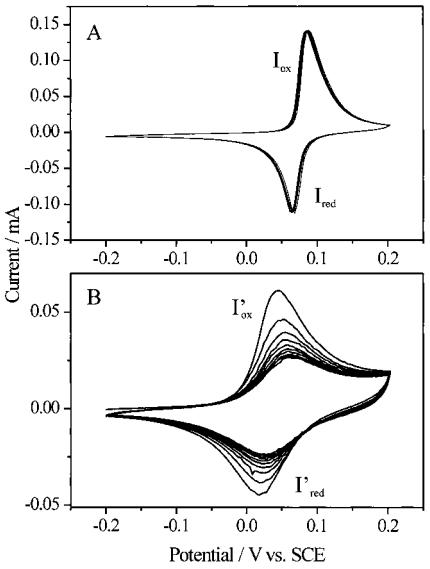

Figure 1. Subsequent cyclic voltammograms for the oxidation of 3.5 nmol THPD (A) and 4 nmol TriHPD (B) deposited on a 4.9 mm diameter basal plane pyrolytic graphite electrode and immersed in a 1 M $NaClO_4$ electrolyte solution with pH = 7.5 and scan rate = 50 mV s^{-1}.

aqueous solution phase is observed (eq 2). This process, denoted I for THPD (I_{ox} and I_{red}) and I′ for TriHPD (I_{ox}' and I_{red}'), can

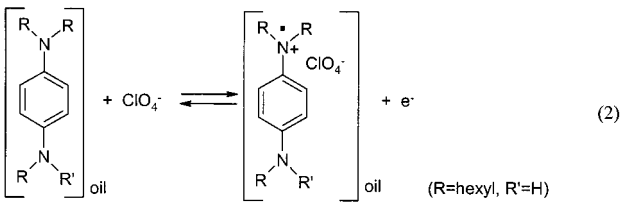

(2)

be detected for both THPD and TriHPD redox liquids (see Figure 1). TriHPD is oxidized at a lower potential, $E_{mid} = 0.04$ V vs SCE, compared to THPD, $E_{mid} = 0.08$ V vs SCE (in 1 M $NaClO_4$). Although the alkyl substituent in THPD may be expected to lower the oxidation potential compared to the hydrogen substituent in TriHPD, better packing of charges in the TriHPD$^+ClO_4^-$ redox liquid is probably responsible for the observed opposite trend. Successive redox cycling of the THPD/THPD$^+ClO_4^-$ system can be seen to result in chemically fully reversible voltammetric responses (Figure 1). However, redox cycling of TriHPD/TriHPD$^+ClO_4^-$ is accompanied by a decay of the voltammetric signal, which especially at slower scan rates of ca. 5 mV s^{-1} leads to a total loss of the current after the first oxidation half-cycle. Electrochemical quartz crystal measurements (see Experimental Section) show that for both, THPD and TriHPD, the frequency of the oscillator returned to its start value after completion of each redox cycle (not shown). This reveals that the mass of compound deposited onto the electrode surface remains approximately constant before and after potential cycling. Thus, the irreversibility detected for TriHPD cannot be attributed to a simple dissolution of compound. It is likely that the hydrolysis of the TriHPD radical cation is responsible for the loss of the electrochemical response. This hydrolysis process[16] may then cause the formation of products, which are not electrochemically active in the potential window used. Support for this interpretation comes from the effect of acid on the voltammetric response for TriHPD, which is consistent with a more reversible process and therefore a slower chemical reaction step at lower pH (vide infra).

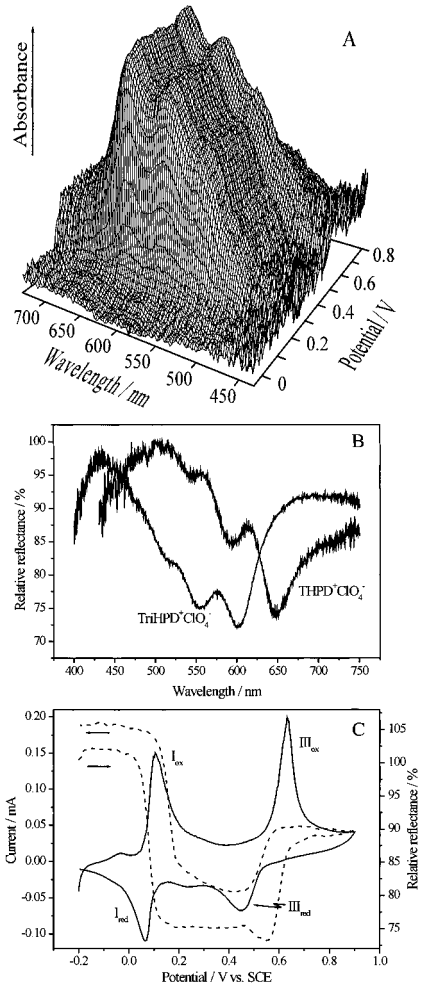

Figure 2. (A) Absorbance spectra of 40 nmol THPD deposited at a planar pyrolytic carbon electrode surface and immersed in a 1 M $NaClO_4$, pH 7, solution. The spectra were recorded in situ during the oxidation half-cycle. (B) Reflectance spectra of THPD$^+ClO_4^-$ and TriHPD$^+ClO_4^-$ produced by the oxidation of the phenylene diamines deposited on the surface of a planar pyrolytic carbon electrode, and immersed into a 1 M $NaClO_4$, pH 7 electrolyte solution. (C) Cyclic voltammogram of the oxidation of a deposit of 40 nmol THPD: trace of the relative reflectance of the electrode surface (λ = 650 nm) recorded in situ during the cyclovoltammetric experiment with 1 M $NaClO_4$, pH = 6.5, and scan rate 10 mV s^{-1}.

The mechanism for the reversible ion insertion and expulsion reaction, which in the case of THPD (Figure 1A) can be observed in a pH range between pH 14 and pH 5 in aqueous 0.1 M $NaClO_4$ also applies for the oxidation of TriHPD (Figure 1B). The radical cation formed for both redox liquids during this oxidation shows very strong light absorption within the visible spectrum, making processes involving these radical cations ideal for spectroelectrochemical investigations. In situ UV/vis reflectance spectroscopy was employed to monitor the redox state of the microdroplet deposits on basal plane pyrolytic graphite electrodes (see Experimental Section). In Figure 2A the change of the reflectance spectra of THPD as a function of the applied oxidation potential obtained with a scan rate of 10 mV s^{-1} is shown. It can be seen that at the oxidation potential of THPD a strong increase of the characteristic absorbance of the THPD deposits occurs. In the monooxidized radical cation state both THPD and TriHPD show absorptions in the 500−650 nm range (see Figure 2B) with maxima at 650 nm and at 605 nm, respectively. In Figure 2C both the voltammetric response and the simultaneously recorded UV/vis trace at 660

nm wavelength are shown. The rapid formation of the radical cation $THPD^+$ at an oxidation potential of 0.05 V can clearly be observed.

At a more positive potential a second redox process is detected (E_{mid} = 0.55 V vs SCE in 1 M $NaClO_4$). This process, denoted III_{ox} and III_{red}, also occurs as a chemically reversible process and can be identified as the second one electron oxidation (eq 3). The voltammetric features of the second

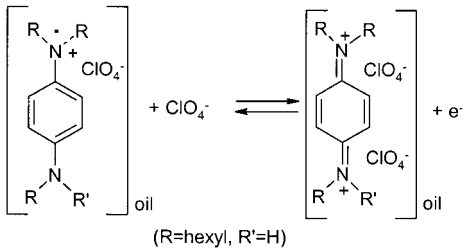

(3)

oxidation (process III), which is accompanied by electroinsertion of a second equivalent of ClO_4^- anions, are different from those of the oil droplet processes. The process is chemically reversible in the presence of perchlorate (eq 3) with a perchlorate-dependent potential shift of $\Delta E_{mid}/\Delta \log a(ClO_4^-) = -55$ mV/log $a(ClO_4^-)$ measured over a range of concentrations from 1 mM to 0.1 M $NaClO_4$. The characteristic potential gap between the oxidation and reduction responses (see Figure 2C) may indicate the formation of a solid phase[17] rather than a liquid product. Further details for this process are under investigation. For TriHPD the chemically reversible reaction according to eq 3 at neutral pH values was not observed. Instead a more complex and chemically irreversible process occurs (not shown).

2. Electrochemically Driven Ion Expulsion from Monoprotonated Tetra- and Trihexylphenylenediamine Ionic Redox Liquids. At a pH values lower than 7 (THPD) or lower than pH 4.5 (TriHPD), an additional redox signal appears, which at pH 4 (THPD) and pH 2.5 (TriHPD) gradually replaces the redox signal associated with processes I and I′. Cyclic voltammetric responses for the oxidation of 1.5 μg (3.5 nmol) of THPD deposited onto a basal plane pyrolytic graphite electrode and immersed in aqueous 1 M $NaClO_4$ electrolyte solution as a function of acid concentration are shown in Figure 3. Processes I and III are readily identified. The additional processes, II_{ox} and II_{red}, detected as reversible responses in the potential range between processes I and III, can be identified as the oxidation and rereduction of the monoprotonated tetrahexylphenylenediamine[10] (eq 4). In this process the protonated redox liquid

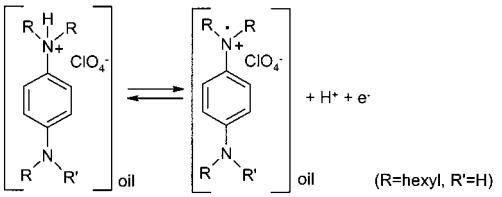

(4)

initially present is ionic and the oxidation and formation of $THPD^+ClO_4^-$ or $TriHPD^+ClO_4^-$ proceeds via expulsion of a proton rather than via anion insertion. Consistent with this mechanism the anticipated shift of the voltammetric response of 59 mV per unit change in pH at 25 °C has been observed ($\Delta E_{mid}/\Delta pH = -63$ mV/pH for THPD and $\Delta E_{mid}/\Delta pH = -56$ mV/pH for TriHPD in the presence of aqueous 0.1 M $NaClO_4$, measured over a range from pH = 4 to 2). As a result, the electrochemical characteristics for process II are very different to those of process I. The voltammetric signals for process II

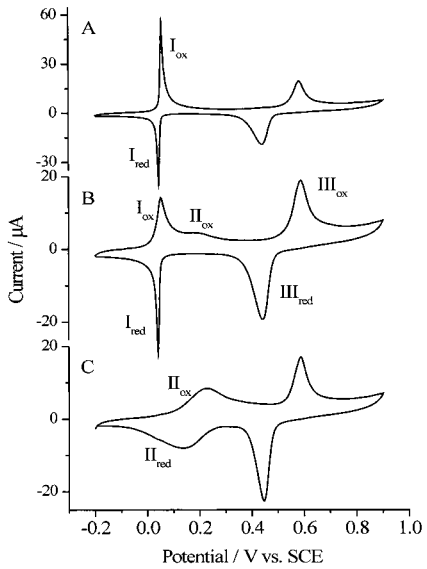

Figure 3. Cyclic voltammograms for the oxidation of 3.5 nmol THPD deposited on a 4.9 mm diameter basal plane pyrolytic graphite electrode and immersed in a 1 M $NaClO_4$ electrolyte solution: (A) pH = 8; (B) pH = 5.9; (C) pH = 3.7. Scan rate = 10 mV s^{-1}.

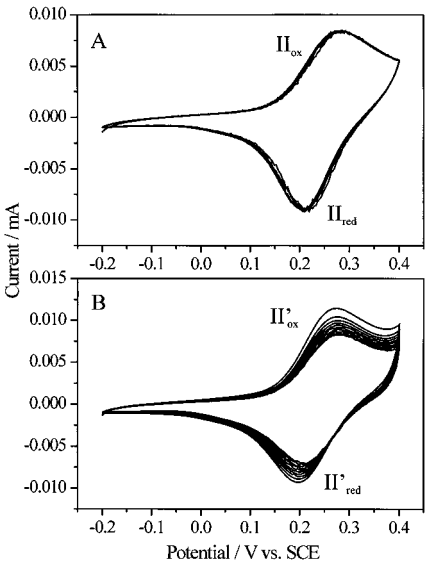

Figure 4. Subsequent cyclic voltammograms for the oxidation of 3.5 nmol THPD (A) and 4 nmol TriHPD (B) deposited on a 4.9 mm diameter basal plane pyrolytic graphite electrode and immersed in a 1 M $NaClO_4$ electrolyte solution with pH = 2.5 and scan rate = 10 mV s^{-1}.

are broad compared to the sharp current peaks observed for process I. Over a pH range of 4.3 to 7 both processes, I and II, may be detected simultaneously. An integration of the peak area of process I_{ox} and process II_{ox} can be used to determine the ratio of neutral versus protonated forms of THPD and TriHPD at a given acid concentration. That is, for sufficiently fast scan rates (ca. 0.05 V s^{-1}) the reequilibration via proton and anion exchange between redox liquid and aqueous phase appears to be slow compared to the electrochemically driven process. Although a detailed explanation for this observation is currently not available, the data obtained voltammetrically allow the equilibrium concentrations in the biphasic protonation process to be quantified on the basis of the integration of the voltammetric responses.

Data plotted in Figure 5 show the integrated charges under the voltammetric responses I_{ox} and II_{ox} in terms of the mole

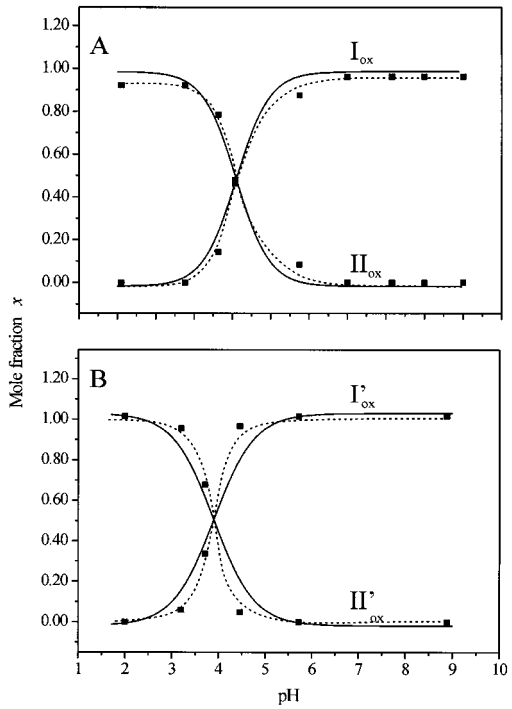

Figure 5. Plot of the mole fraction x versus pH showing the dependence of the extent of ionic liquid formation due to redox processes I and II of THPD (A) and I′ and II′ of TriHPD (B). Data were obtained from peak analysis of cyclic voltammograms of the oxidation of deposited 4 nmol redox liquid. Scan rate = 10mV s^{-1}, with 1 M $NaClO_4$, and pH was adjusted with $HClO_4$ and NaOH. The dashed lines represent the actual fits derived from the experimental data. The solid lines were derived from eq 5.

fraction as a function of pH. A dashed line is indicating the best fit through the experimental data whereas a solid line indicates the theoretical line based on ideal behavior as expressed in eq 5, which has been adapted from the treatment usually applied to monophasic acid−base equilibria.[18]

$$\log\left(\frac{1}{x} - 1\right) = \mathrm{p}K_{\mathrm{A}} - \mathrm{pH} \qquad (5)$$

In this expression the mole fraction x = (moles of oxidized material)/(moles of deposit) is a function of the acid−base equilibrium constant, K_A, and the proton concentration. For the biphasic system the protonation is accompanied by the simultaneous transfer of an anion from the aqueous into the organic phase. However, the use of an equilibrium constant describing the overall process is possible and a comparison to conventional protonation processes is possible. Any deviation from ideal behavior or immiscibility of the protonated and neutral forms of the redox liquid would become apparent from the shape of the plot of mole fraction against solution pH deviating from the behavior predicted by eq 5. Surprisingly, deviations of the experimental data for the biphasic system from ideal behavior can be seen to be relatively small (Figure 5). From the intersection of the curves of the molar fractions of the protonated and the unprotonated compounds well-defined $pK_{A2,biphasic}$ values can be determined as $pK_{A2,biphasic} = 5.1$ for THPD and $pK_{A2,biphasic} = 3.9$ for TriHPD in the presence of 1 M perchlorate. Due to the impact of the Gibbs free energy of the transfer of the anions between the aqueous and the organic phase these values are sensitive to the nature of the anion present.[10] It is interesting to compare the $pK_{A,biphasic}$ values with estimated pK_A values predicted for the protonation in a homogeneous aqueous environment. Estimates (based on the extrapolation of the pK_A from a database[19]) which reflect the effect of the additional alkyl substituent in THPD replacing the hydrogen substituent are $pK_{A2} = 7.5 \pm 0.5$ for THPD and $pK_{A2} = 8.8 \pm 0.5$ for TriHPD.[19] Obviously, the trend in pK_A values in the biphasic medium is opposite to that anticipated for an aqueous solution, and this may be rationalized in terms of a dominating cation−anion intermolecular interaction, which in the biphasic system is more important than the intramolecular proton−base interaction.

In contrast to the ClO_4^- anion insertion processes observed for THPD, process I ($E_{mid} = 0.075$ V vs SCE), and for TriHPD, process I′ ($E_{mid} = 0.035$ V vs SCE), in the presence of 1 M aqueous sodium perchlorate electrolyte solution, processes II and II′ were found to take place at essentially identical formal potentials ($E_{mid} = 0.245$ V vs SCE) for both compounds, THPD and TriHPD. Also the shape of both voltammetric responses is very similar (see Figure 5) suggesting an overall very similar mechanism. The similar mid potential for both processes suggests that the energetics for the transfer of protons from the aqueous electrolyte into the ionic redox liquid upon reduction is not dominated by the difference in the protonation constants between THPD and TriHPD.

Whereas the oxidation of THPD is chemically fully reversible (decrease of peak currents <2% during 20 redox cycles at a scan rate of 10 mV s^{-1}), the radical cation of TriHPD undergoes a follow-up reaction leading to decreasing voltammetric signals. It can be seen from a comparison of Figure 1B and Figure 4B that the loss of electrochemical signal for the TriHPD deposit is slowed remarkably with decreasing pH value. This finding supports the assumption that the decomposition of the radical cation of TriHPD proceeds via a hydrolysis reaction involving the monohexylamine substituent.[16] The oxidation of TriHPD to the radical cation at pH values greater than pH > 8 becomes totally chemically irreversible.

A closer inspection of the reaction mechanism suggests that the oxidation of the protonated and the unprotonated forms of the redox liquids may proceed through different pathways. In the unprotonated state, THPD and TriHPD are likely to be good electronic and ionic insulators. Thus, an electrochemical reaction can only be initiated at the three phase junction electrode|oil|aqueous solution, where charge compensation within the redox liquid can be realized and from which the reaction can progress into the droplet deposit. For the case of deposits of microdroplets of THPD, this process has been visualized[9] by light microscopy. The assumption of an initiation of the oxidation at the three-phase junction implies that the modification of the electrode surface with a continuous film of THPD or TriHPD would not allow the oxidation to take place. Experimental results confirm this assumption. In the presence of a 0.1 M sodium perchlorate electrolyte solution (at pH 7) and a continuous layer of the redox liquid THPD (ca. 10 μm thickness) the reaction is fully inhibited. A reaction could be observed only when the layer of THPD did not fully cover the electrode surface and graphite was exposed e.g. at the edges of the graphite electrode. Figure 6A illustrates this phenomenon for the case of the formation of the colored TriHPD radical cation. It shows the photographic image of an imprint of a graphite electrode surface modified with a layer of TriHPD after electrolyzing the deposit at an applied potential of 0.2 V vs SCE for 30 s. The oxidation product is formed starting only from the three-phase junction at the edge of the electrode, from which the reaction advances into the center of the layer (see also Figure 7A). As the reaction product represents an ionic conductor, it can be assumed that the reaction zone grows as

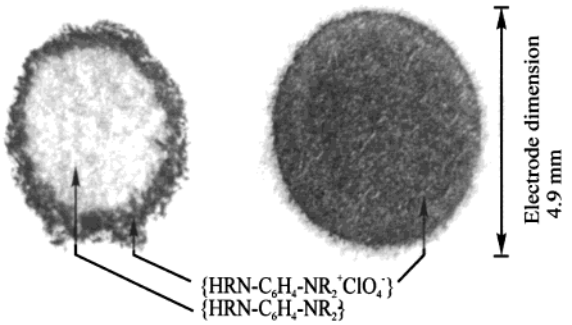

Figure 6. Photographic image of a stamp imprint of the interface layer of TriHPD at a graphite electrode. The electrode was modified with a closed layer of the redox liquid and electrolyzed at a potential of +0.5 V vs SCE for 60 s in order to form the colored radical cation.

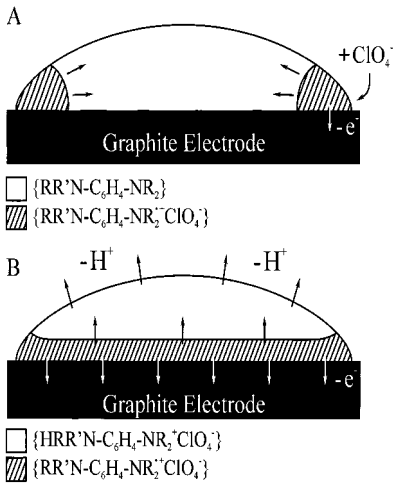

Figure 7. Schematic drawing of the mechanism of the oxidation of deposits of (A) a neutral redox liquid and (B) an ionic redox liquid.

the reaction advances and product is formed. A related type of an insertion−electrochemical reaction has been described theoretically[20] for the case of a reaction of a solid compound.

The requirement for the initiation of the reaction at the three-phase junction does not apply for the oxidation of the protonated redox liquid in the presence of an acidic aqueous solution phase. At pH values where the substrate is protonated (see eq 1) the oxidation of the deposit can be initiated even in the case of a continuous layer of TriHPD or THPD. The product is formed at the entire electrode surface, leaving a homogeneous film of the reaction product (Figure 6B). The protonation reaction, which is accompanied by a simultaneous uptake of protons and anions into the bulk of the organic oil, converts the neutral redox liquid into an ionic conductor allowing charge compensation at the entire electrode|oil interface, as shown in the schematic drawing in Figure 7B. For applications such as in energy storage systems or electrochromic devices the use of ionic redox liquids may be advantageous over neutral redox liquid systems due to the lack of triple-interface restrictions. In the case of a neutral redox liquid a structured or highly porous electrode material has to be employed in order to maximize the triple-interface reaction zone.

3. Electrochemically Driven Ion Insertion in Tetra- and Trihexylphenylenediamine Redox Liquids in the Presence of Strong Acid. Both THPD and TriHPD have two amine substituents and therefore may be protonated twice. The higher the concentration of protons in the electrolyte solution, the more the mid potential for the voltammetric response associated with the electrochemically driven proton expulsion process (eq 4) is

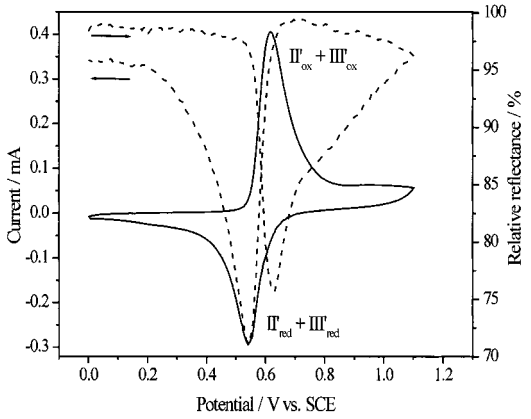

Figure 8. Cyclic voltammogram of the oxidation of a deposit of TriHPD with 2.5 M $HClO_4$: trace of the relative reflectance of the electrode surface ($\lambda = 600$ nm) recorded in situ during the cyclovoltammetric experiment with scan rate 10 mV s^{-1}.

shifted positive. Therefore, with increasing acid concentration the potential gap between processes II and III gradually decreases. In the case of THPD the presence of strong acid (aqueous $HClO_4$) is not leading to the detection of new voltammetric signals. Instead, the second protonation step, which was found to take place at pH values lower than 1.5, was found to lead to rapid dissolution of the more soluble diprotonated species.

Surprisingly, for TriHPD up to concentrations of 2.5 M $HClO_4$ no second protonation step could be observed, although the first protonation step is observed more readily for TriHPD compared to THPD. This result could be interpreted in terms of intermolecular hydrogen bonding between the sterically less crowded monoprotonated TriHPD molecules. For TriHPD the increasing concentration of protons in the electrolyte solution finally leads to a superposition of the redox processes II and III (Figure 8). This results in a situation in which two different ion transfer steps, the release of protons (first oxidation) and the uptake of perchlorate anions (second oxidation), take place apparently simultaneously at the same potential. As Figure 8 shows by means of the trace of the change of the reflectance the colored radical cation is formed and almost immediately consumed. The experiment proves that both oxidation reactions take place at this potential and that indeed a consecutive process occurs with a TriHPD radical cation intermediate rather than the simultaneous two electron conversion.

The superposition of the first and the second oxidation steps of TriHPD leads to an increased chemical reversibility of the oxidation of TriHPD. This may be attributed to both the short lifetime of the radical cation, which is consumed immediately in the second redox step before undergoing follow-up reactions and the high concentration of acid.

Conclusions

Electrochemical processes in thin film and droplet deposits of THPD and TriHPD have been investigated as a function of the proton concentration in the aqueous electrolyte. On the basis of the voltammetric and in-situ spectroelectrochemical experiments, it has been shown that both neutral and ionic redox liquids undergo redox conversion accompanied by ion insertion or expulsion. However, mechanistically they differ considerably due to the lack of ion conductivity in the neutral redox liquid. Ionic redox liquids undergo electrochemical processes in the absence of triple phase boundaries and are therefore independent of the type and morphology of the electrode. The investigation

of properties such as the biphasic protonation constants and mid potentials for redox conversions of redox liquids revealed that intermolecular factors may dominate over intramolecular factors due to direct interactions in the absence of a solvent.

Acknowledgment. U.S. gratefully acknowledges support from the Alexander von Humboldt foundation (Feodor Lynen Program). F.M. thanks the Royal Society for a University Research Fellowship and New College, Oxford, U.K., for a Stipendiary Lectureship.

References and Notes

(1) See for example: Girault, H. H. In *Modern Aspects of Electrochemistry*; Bockris, J. O'M., Conway, B. E., White, R. E., Eds.; Plenum Press: New York, 1993; Vol. 25, p 2.

(2) Shi, C. N.; Anson, F. C *J. Phys. Chem. B* **1999**, *103*, 6283.

(3) Scholz, F.; Komorsky-Lovric, Š.; Lovric, M. *Electrochem. Commun.* **2000**, *2*, 112.

(4) Scholz, F.; Meyer B. *Chem. Soc. Rev.* **1994**, *23*, 341.

(5) See for example: Shouji, E.; Buttry, D. A. *Langmuir* **1999**, *15*, 669.

(6) See for example: Laforgue, A.; Simon, P.; Sarrazin, C.; Fauvarque, J. F. *J. Power Sources* **1999**, *80*, 142.

(7) See for example: Hermes, M.; Scholz, F. *J. Solid State Electrochem.* **1997**, *1*, 215.

(8) Marken, F.; Blythe, A.; Compton, R. G.; Bull, S. D.; Davies, S. G. *Chem. Commun*. **1999**, 1823.

(9) Marken, F.; Webster, R. D.; Bull, S. D.; Davies, S. G. *J. Electroanal. Chem.* **1997**, *437*, 209−218.

(10) Marken, F.; Compton, R. G.; Goeting, C. H.; Foord, J. S.; Bull, S. D.; Davies, S. G. *Electroanalysis* **1998**, *10*, 821.

(11) Wadhawan, J. D.; Compton, R. G.; Marken, F.; Bull, S. D.; Davies, S. G. *J. Solid State Electrochem.* **2000**, in press.

(12) See for example: Ward, M. D. In *Physical Electrochemistry, Principles, Methods, and Applications*; Rubinstein I., Ed.; Marcel Dekker: New York, 1995; p 293.

(13) See for example: Shaw, S. J.; Marken, F.; Bond, A. M. *J. Electroanal. Chem.* **1996**, *404*, 227.

(14) Oldham, K. B. *J. Solid State Electrochem*. **1998**, *2*, 367.

(15) Ball, J. C.; Marken, F.; Fulian, Q.; Wadhawan, J. D.; Blythe, A. N.; Schroeder, U.; Compton, R. G.; Bull, S. D.; Davies, S. G. *Electroanalysis* **2000**, *12*, 1017.

(16) Adams, R. N. *Electrochemistry at Solid Electrodes*, Marcel Dekker: New York, 1969; p 356.

(17) Bond, A. M.; Fletcher, S.; Marken, F.; Shaw, S. J.; Symons, P. G. *J. Chem. Soc., Faraday Trans.* **1996**, *92*, 3925.

(18) See for example: de Levie, R. *Aqueous Acid-Base Equilibria and Titrations*; Oxford University Press: Oxford, U.K., 1999; p 4.

(19) Obtained from http://www.acdlabs.com/.

(20) Schröder, U.; Oldham, K. B.; Myland, J.; Mahon, P. J.; Scholz, F. *J. Solid State Electrochem.* **2000**, *4*, 314.